Int. J. Electrochem. Sci., 13 **(2018)** 6426 – 6435, doi: 10.20964/2018.07.48

International Journal of ELECTROCHEMICAL SCIENCE
www.electrochemsci.org

Synthesis, Characterization and Electrochemical Properties of α-MnO_2 Nanowires as Electrode Material for Supercapacitors

Hidayat Ullah Shah[1], Fengping Wang[1,], Muhammad Sufyan Javed[2,3], Rabia Saleem[4], Muhammad Shahzad Nazir[5], Jinbing Zhan[1], Zia Ul Haq Khan[6], Muhammad Umer Farooq[7], Shujaat Ali[1]*

[1] Department of Physics, School of Mathematics and Physics, University of Science and Technology Beijing, Beijing 100083, P. R. China
[2] Siyuan Laboratory, Guangzhou Key Laboratory of Vacuum Coating Technologies and New Energy Materials, Guangdong Provincial Engineering Technology Research Center of Vacuum Coating Technologies and New Energy Materials, Department of Physics, Jinan University, Guangzhou 510632, People's Republic of China
[3] Department of Physics, COMSATS University, Lahore 54000, Pakistan
[4] Department of Mathematics, COMSATS University, Lahore 54000, Pakistan
[5] Energy Research Institute, School of Electrical Power, South China University of Technology, Guangzhou 510640, People's Republic of China
[6] Department of Environmental Sciences, COMSATS University, Vehari 61100, Pakistan
[7] School of Materials Science and Engineering, University of Science and Technology Beijing, Beijing 100083, China
[*]E-mail: fpwang@ustb.edu.cn

Received: 5 March 2018 / *Accepted:* 6 May 2018 / *Published:* 5 June 2018

High purity α-MnO_2 rectangular nanowires are synthesized by a facile one-step hydrothermal method. The morphology and composition of α-MnO_2 nanowires are characterized by X-ray diffraction, energy-dispersive X-ray spectroscopy (EDX), Field emission scanning electron microscopy (FESEM), X-ray photoelectron spectroscopy (XPS) and Fourier transform infrared (FTIR) spectral techniques. The electrochemical properties of α-MnO_2 nanowires have been studied as electrode material for supercapacitors. The α-MnO_2 nanowires exhibit a high specific capacitance of 362 Fg^{-1} at a current density of 1.0 Ag^{-1} with a good cycling stability (maintained 83% after 5000 cycles). These results indicate its promising applications as a high-performance electrode material for electrochemical energy storage.

Keywords: Hydrothermal; MnO_2; Nanowires; Supercapacitors: Electrodes

1. INTRODUCTION

Global warming is the biggest threats human facing in the 21st century, and sea levels are continuing to rise at alarming scales. The pollution produced due to ignition of fossil fuel has created

major environmental problems across the globe [1]. Cleaned renewable energy sources are highly necessary for our modern society [2]. Energy storage creates new ideas to use energy cleanly and efficiently. Electrochemical capacitors (ECs) also known as supercapacitors (SCs) are a new type of energy storage/conversion device. Recently, SCs have received massive attention due to their longer cycle life, higher power density, quick charging compared to conventional batteries and higher energy density than typical electrical double-layer capacitors (EDLC) [3]. In general, SCs possess several desirable features, including environmental friendliness, good efficiency, high safety, and can be used in a high-temperature range with almost infinite long cycle life and low maintenance [4]. Thus, SCs have been applied in transportation, electronics, communications, aviation, and associated technologies in and have shown potential applications [5,6].

Manganese dioxides (MnO_2) have been regarded as the best electrode material because of its low cost, natural abundance, low toxicity and wide voltage range [7,8]. MnO_2 exists in different crystalline forms, such as α, β, γ and δ-types, made of the basic unit [MnO_6] octahedron [9]. Among these crystallographic structures, α-MnO_2 appears to be the most favourable electrode materials for supercapacitor applications because of its wide tunnel size of 0.46 nm which enhanced its diffusion and capacitance capabilities. As supercapacitors mostly depend on either the interlayer separations between sheets of MnO_6 octahedral or the sizes of the tunnels, different tunnel structures have distinct proficiencies for ion transmission, α-MnO_2 2 x 2 (4.6 x 4.6 Å) tunnels constructed from double chains of octahedral [MnO_6] structure have appropriate gaps to accommodate these ions [10]. The electrode materials with proper nanostructures greatly depend and enhance the rate capability and stability upon repeated charge/ discharge of the SCs [11]. One-dimensional (1-D) nanostructures having controlled sizes and crystalline structure offer extra active sites for electrochemical reactions, shorten the diffusion paths for both electrons and ions in the presence of oxides, and then enhance electrochemical properties of the electrodes [12,13].

In this study, we have synthesized 1-D α-MnO_2 nanowires material via a simple hydrothermal method. These 1-D thin-walled α-MnO_2 nanowires have higher specific capacitance of 362 Fg^{-1} at a current density of 1.0 Ag^{-1}. The results given below will be able to understand the detailed synthesis, morphology, structural and electrochemical properties of α-MnO_2.

2. EXPERIMENTAL DETAILS

2.1. Chemical

All the chemical used were of analytical grade and used without any additional refinement. Potassium permanganate ($KMnO_4$), nitric acid (HNO_3) and tin oxide (SiO_2) were purchased from local Beijing market.

2.2. Material syntheses

In order to study the growth mechanism of α-MnO_2 nanowires, 3 g of pure $KMnO_4$ was added to 45 ml of deionized water (DI) and magnetically stirred for 15 minutes. During the stirring process,

0.5 ml HNO_3 and 0.2 g of SiO_2 were added and further stirred for another 20 minutes. The final solution was transferred to a stainless autoclave and heated at 180 °C in electric oven for 24 hours (h). After the reaction, the as-prepared samples were washed, filtered and dried at 120 °C for 4 h in an oven. SiO_2 was used as a catalyst. The final product was collected for further characterizations. The growth mechanism of the synthesis process is shown figure 1.

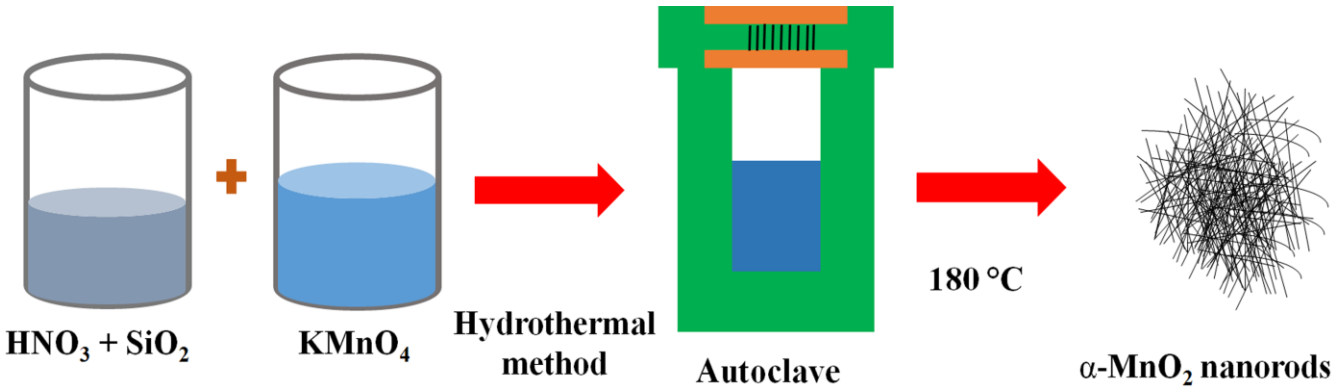

Figure 1. Schematic diagram showing the synthesis process of α-MnO_2 nanowires

2.3. Characterizations

XRD data was taken with X-ray diffractometer (X'Pert MPD-XRD) with Cu-Kα radiation (λ= 0.154nm). The morphological investigation of the samples was carried out by field emission scanning electron microscope (FESEM, ZEISS 55), transmission electron microscope (TEM), high-resolution transmission electron microscopy (HRTEM), selected area electron diffraction (SAED JEM 2010), energy dispersive spectroscopy (EDS, OXFORD 51-XMX) and selected area electron diffraction (SAED JEM 2010). X-ray photoelectron spectroscopy (XPS) was carried out by AXIS ULTRA^{DLD}. A Fourier transform infrared (FTIR) spectrum was recorded on a Bruker Vector 33 spectrometer.

2.4. Electrode preparation and electrochemical characterization

The working electrode was prepared by mixing 75 wt% active material (α-MnO_2 powder), 15 wt % conducting filler of acetylene black and 10 wt % polyvinylidene fluoride (PVDF) in the presence of few drops of water. The final slurry was pasted onto a nickel foam (width x length = 1 × 2 cm^2) current collector.

The electrochemical properties of the α-MnO_2 electrode were measured on the CHI660C electrochemical workstation. The cyclic voltammetry (CV) and galvanostatic charging/discharging (GCD) techniques were used to study the electrochemical performance of the electrode. The CV was recorded in a potential window range from -0.1 V to 0.9 V at different scan rates. The GCD experiment was recorded at different current densities between a potential range from 0.0 V and 0.5 V. The mass loading density of the active material in the electrode was about 1.5 mg cm^{-2}.

The specific capacitance was calculated by the following equation [14].

$$C_s = \frac{I\,\Delta t}{\Delta V m} \qquad (1)$$

Where C_s stand for specific capacitance (F g^{-1}), I is the discharge current, Δt is the discharge time (s), ΔV is the potential drop (V), and m is the active mass of the active electrode (g).

3. RESULTS AND DISCUSSION

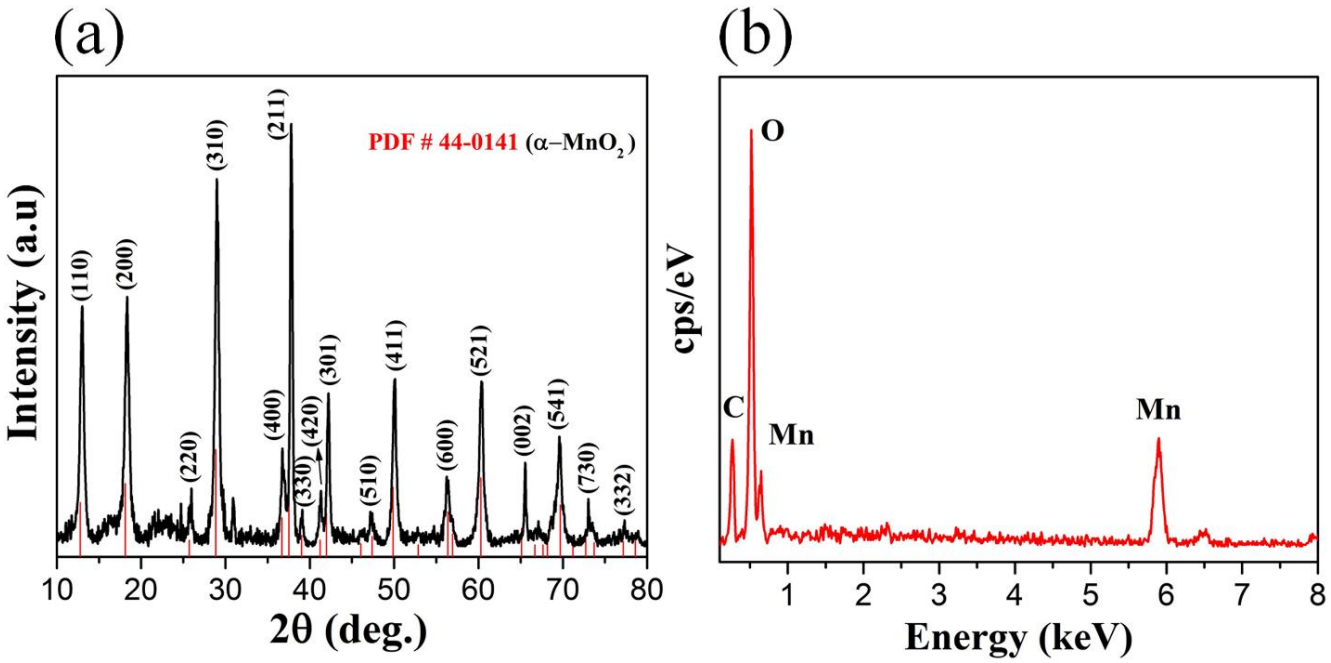

Figure 2. (a) Typical XRD and (b) EDX spectra of the as-prepared α-MnO_2 products.

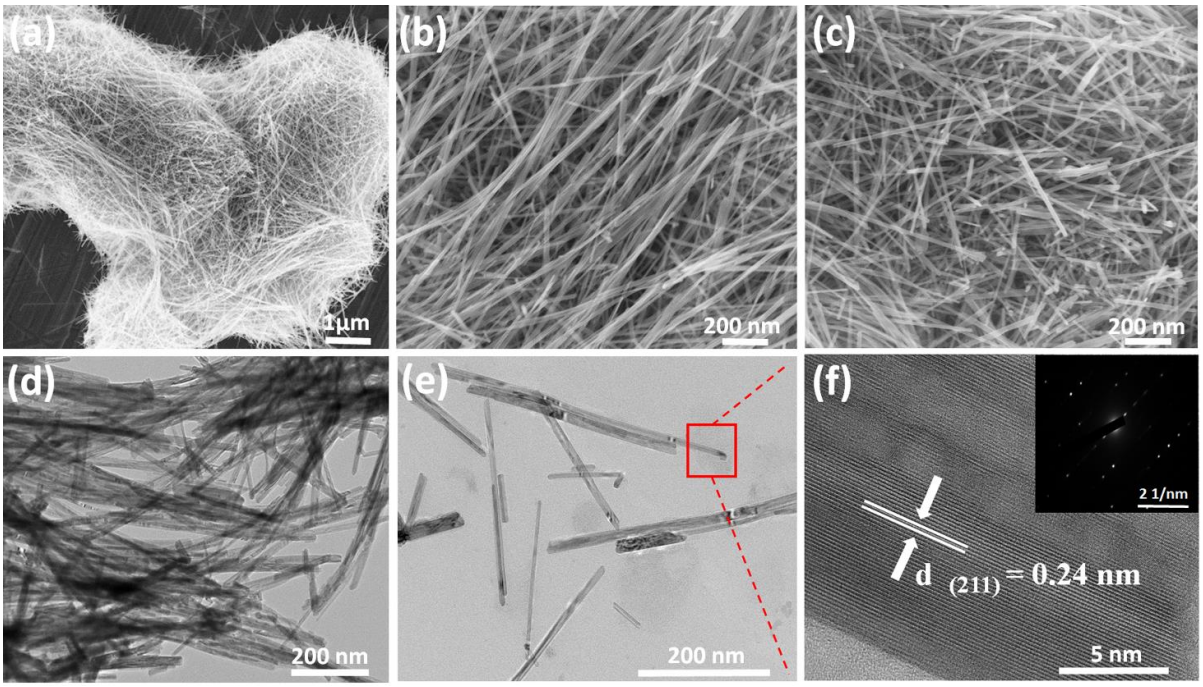

Figure 3. (a-c) FESEM; (d,e) TEM and (f) HRTEM images of the α-MnO_2 nanowires; the inset shows the related SAED pattern of the individual α-MnO_2 nanowires.

The phase purity and crystalline structure of the samples have been characterized by XRD, presented in Figure 2(a). All the peaks are well indexed to the standard value (JCPDS: 44 - 0141) [15]. The diffraction peaks can be absolutely indexed as the tetragonal α-MnO_2, and no other peaks were observed from impurities. The sharp and narrow diffraction peaks indicate the high crystallinity of α-MnO_2 material. EDX analysis of the sample depicted in Figure 2(b) exhibits that the final product comprises of only Mn and O, suggesting that the nanowires are made of pure α-MnO_2. There is carbon (C) peak in the EDX spectra which comes from Ethanol, during the sample preparations.

The morphological properties of the as-prepared α-MnO_2 nanowires were studied by FESEM, TEM and HRTEM as shown in Figure 3. Figure 3 (a-c) shows the FESEM micrograph of α-MnO_2 nanowires, all the images confirm the uniform formation of α-MnO_2. The TEM images are shown Figure 3(d,e), which exhibits single-crystal structure of α-MnO_2 nanowires. Figure 3(f) shows the HRTEM image of the nanowires. This figure shows clear lattice fringes, verifying the single-crystalline nature of the as-synthesized material. The interplanar spacing (*d*) of 0.24 nm corresponds to the [211] plane of tetragonal α-MnO_2.

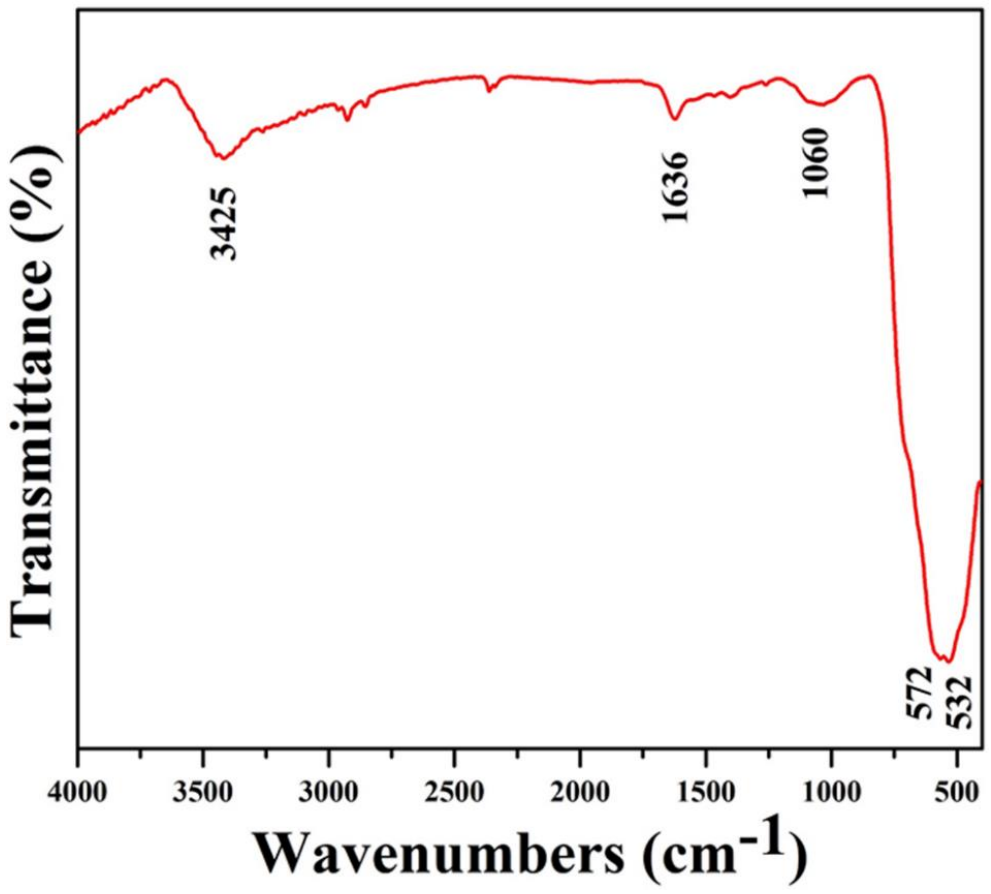

Figure 4. FTIR spectra of the as-prepared α-MnO_2 nanowires

FTIR technique was used for the samples shown in Figure 4. The spectrum was recorded in the range of 500-4000 cm^{-1}. The absorption bands were found at 532, 572, 750, 1060, 1636 and 3425 cm^{-1}. The broad absorption bands at 3425 $cm^{-1}$and 1060 cm^{-1} represent O–H stretching vibration and

bending vibration absorption peaks of residual water on MnO_2 surface. The band around 1636 cm^{-1} assigned to vibrations in carbonyl groups (C–O) [16]. The bands at about 532 and 572 cm^{-1} can be ascribed to the Mn–O stretching mode of the octahedral layers in MnO_2. This result is consistent with the previous results in the literature [17,18].

XPS is a surface analytical technique with a sampling depth of around 10 nm. The XPS study investigates the oxidation state of Mn within the α-MnO_2, shown in Figure 5, exhibiting signals from Mn, C, and O elements, corresponds to the EDX results. The existence of MnO is proved by Mn 3s, Mn 2p and O 1s peaks. The Mn 2p peak shown in Figure 5(b) further consists of the spin-orbit doublet of Mn $2p_{1/2}$ and Mn $2p_{3/2}$ located at 653.3 and 641.5 eV, respectively. The spin-energy separation of 11.8 eV suggests the formation of MnO_2 [19,20]. Figure 5 (c,d) further explains C and O peaks.

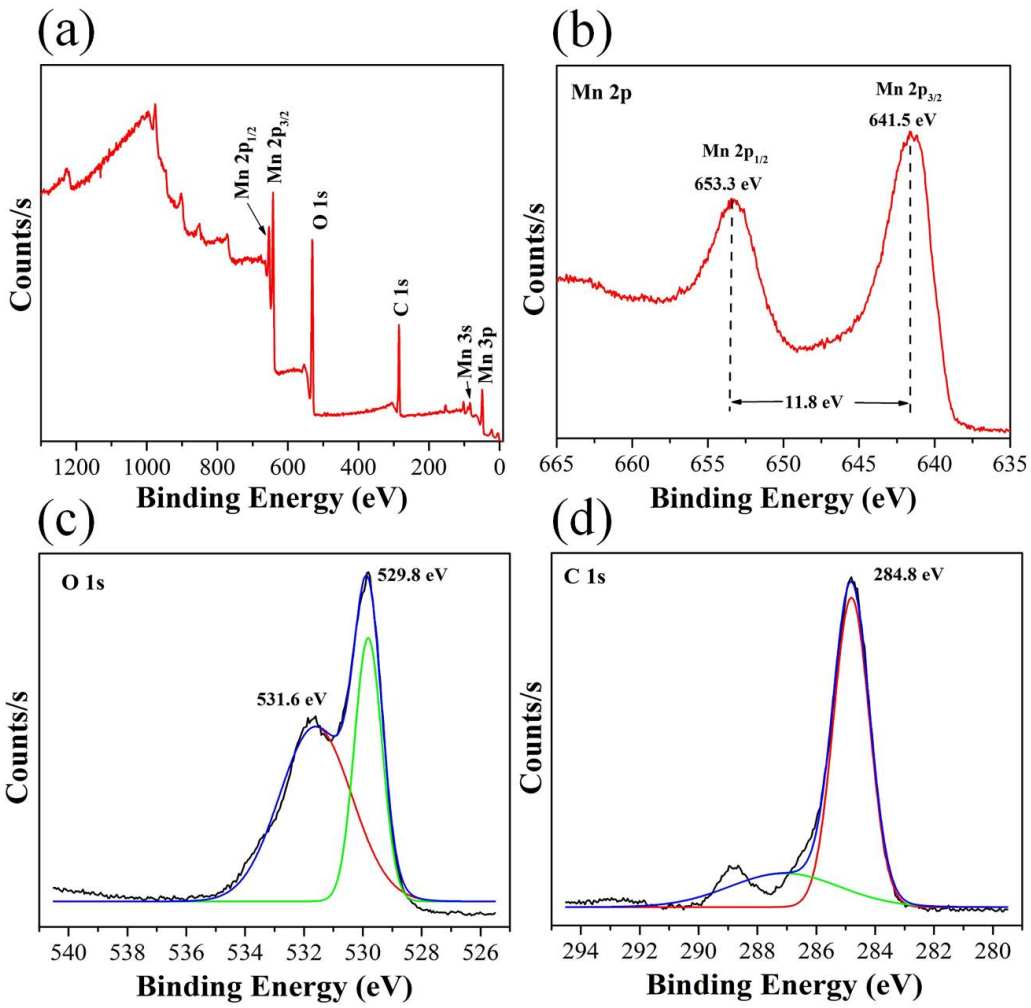

Figure 5. (a) XPS spectrum (survey scan) of the α-MnO_2; magnified view of the (b) Mn 2p (c) O 1s and (d) C 1s levels.

3.1. Electrochemical characterization

To investigate the potential applications of α-MnO_2 as electrode materials for supercapacitor, CV curves, GCD curves and EIS spectra are tested by a three-electrode system in 1 M Na_2SO_4 aqueous

electrolyte and the results are shown in Figure 6, in which platinum wire and Ag/AgCl electrodes were used as the counter and reference electrodes, respectively. The curves of α-MnO_2 SCs electrode are measured at different scan rates within a voltage windows ranging from 0 to 0.8 V. The CV curves are composed of a rectangular and symmetric shape, showing its typical pseudo-capacitive nature with fast charge/discharge reaction. CV curves of the α-MnO_2 are measured at a scan rate ranging from 10 to 200 mV s^{-1} are shown in Figure 6(a-b). The curves exhibit rectangular shapes even at higher scan rate (200 mV s^{-1}) without seeing any additional redox peaks. Figure 6(c) shows GCD results of the electrode at different current densities (1, 1.5, 2, 2.5, 3 and 4 Ag^{-1}) in the potential range of 0.0 to 0.5 V versus Ag/AgCl. The specific capacitance as function of current densities is shown in Figure 6(d). The specific capacitances of 362, 263, 175, 131, 79 and 40 Fg^{-1} were evaluated at a current density of 1, 1.5, 2, 2.5, 3 and 4 Ag^{-1}, respectively. The specific capacitance decreased from 362 to 40 Fg^{-1} when the current density increased from 1 to 4 Ag^{-1}. The specific capacitance had a lower value at a higher current density because the electrolyte ions did not have sufficient time to diffuse in and out of the interior surface of the active material [21]. The obtained capacitance is higher than other reported MnO_2 supercapacitors electrodes shown in Table I.

Table I. Specific capacitances (C_s) of MnO_2 materials and other related reports under different morphology electrodes.

Materials		Electrolyte	Cs ($F.g^{-1}$)	Current density or scan rate	Ref.
1	α-MnO_2 nanowires	1.0 M Na_2SO_4	362	1.0 Ag^{-1}	This work
2	MnO_2 /GO	1.0 M Na_2SO_4	360	2.5 Ag^{-1}	[11]
3	MnO_2/exfoliated graphite	1.0 M Na_2SO_4	358	2 mV s^{-1}	[22]
4	MnO_2 nanoparticles	1.0 M $Ca(NO_3)_2$	282	0.5 mA cm^{-2}	[23]
5	hierarchical MnO_2	1.0 M Na_2SO_4	202.6	0.25 Ag^{-1}	[24]
6	α-MnO_2 nanorods	1.0 M Na_2SO_4	198	1.0 Ag^{-1}	[9]
7	amorphous MnO_2	1.0 M NaCl	110	5 mV s^{-1}	[25]

The cycling stability of the α-MnO_2 electrodes was investigated by subjecting them to repeated charge-discharge process. The cycling process was performed at a current density of 2 A/g for 5000

cycles. The variation of specific capacitance as a function of cycle number is shown in Figure 6(e). It can be noticed that the specific capacitance of α-MnO_2 electrodes maintains about 83 % of its initial value after 5000 cycles.

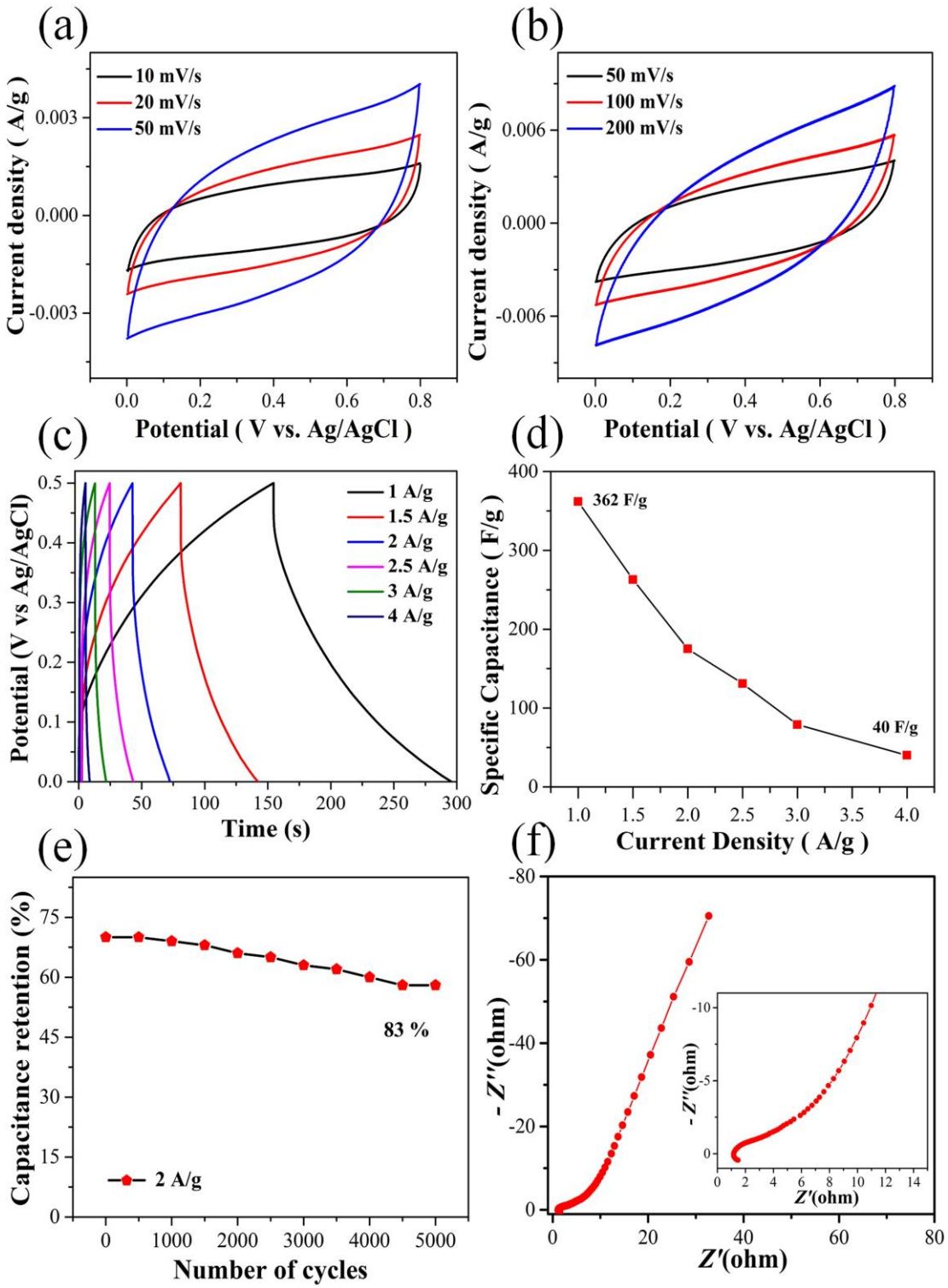

Figure 6. (a-b) CV curves at various scan rates; (c) GCD curves at different current densities ranging from 1 to 4 Ag^{-1}; (d) specific capacitances at different current densities; (e) cycling life of electrode; (f) Impedance spectra of the as-prepared α-MnO_2 electrode.

The EIS analysis has been shown in shown in Fig. 6(f). The impedance spectrum consists of semicircle at higher frequencies, representing the interfacial Faradic charge transfer resistance (R_{ct}), showing the resistance of the electrochemical reactions at the surface of electrode. The vertical line ensures the better capacitive performance of α-MnO_2 electrode. The straight sloping R_{ct} line indicates the pure capacitive behaviour. The α-MnO_2 nanowires electrode has smaller R_{ct} value 1.4 Ω. The low values of R_{ct} show superior charge transfer performance of electrode [26].

4. CONCLUSIONS

In summary, α-MnO_2 nanowires have been successfully synthesized via simple hydrothermal method. The capacitive performances of α-MnO_2 nanowires electrode show the higher specific capacitance of 362 Fg^{-1} at a current density of 1.0 Ag^{-1}, excellent rate capability and long-term cycling stability. Based on the investigation of the chemical structure, morphology, and electrochemical behaviour of α-MnO_2 nanowires, we achieved higher specific capacitance. These results suggest that this material will have potential applications in sensors, power sources, and other nano-devices, etc.

ACKNOWLEDGEMENTS
We appreciate the financial support of the National Natural Science Foundation of China (Grant No. 61373072).

References

1. M. Huang, Y. Zhang, F. Li, L. Zhang, R.S. Ruoff, Z. Wen, *Sci. Rep.*, 4 (2014) 3878.
2. M. Armand, J.-M. Tarascon, *Nature.*, 451 (2008) 652.
3. P. Simon, Y. Gogotsi, *Nat. Mater.*,7 (2008) 845.
4. A.S. Aricò, P. Bruce, B. Scrosati, J.-M. Tarascon, *Nat. Mater.*, 4 (2005) 366.
5. S. Hussain, T. Liu, M.S. Javed, N. Aslam, N. Shaheen, *Ceram. Int.*, 42 (2016) 11851.
6. C. Choi, K.M. Kim, K.J. Kim, X. Lepró, G.M. Spinks, *Nat. Commun.*, 7 (2016) 13811.
7. H.U. Shah, F. Wang, M.S. Javed, N. Shaheen, M. Saleem, *Ceram. Int.*, 44 (2017) 3580.
8. Y. Yuan, C. Zhan, K. He, H. Chen, W. Yao, S. Sharifi-Asl, *Nat. Commun.*, 7 (2016) 13374.
9. W. He, W. Yang, C. Wang, X. Deng, B. Liu, *Phys. Chem. Chem. Phys.*, 18 (2016) 15235.
10. N. Kijima, T. Ikeda, K. Oikawa, F. Izumi, *J. Solid State Chem.*, 177 (2004) 1258.
11. Y. Haldorai, K. Giribabu, S.K. Hwang, C.H. Kwak, *Electrochim. Acta.*, 222 (2016) 717.
12. H.U. Shah, F. Wang, M. Sufyan, M.A. Ahmad, M. Saleem, *J. Energy Storage.*, 17 (2018) 318.
13. L. Li, C. Nan, J. Lu, Q. Peng, Y. Li., *Chem. Commun.*, 48 (2012) 6945.
14. H. U. Shah, F.P.Wang, *Int. J. Electrochem. Sci.*, 11 (2016) 8155.
15. W. Li, R. Zeng, Z. Sun, D. Tian, S. Dou, *Sci. Rep.*, 4 (2014) 6641.
16. Y. Jiang, X. Ling, Z. Jiao, L. Li, Q. Ma, M. Wu, Y. Chu, *Electrochim. Acta.*, 153 (2015) 246.
17. L. Bao, X. Li, *Adv. Mater.*, 24 (2012) 3246.
18. M. Tian, M. Du, L. Qu, K. Zhang, H. Li, S. Zhu, D. Liu, *J. Power Sources.*, 326 (2016) 428.
19. M. Huang, Y. Zhang, F. Li, Z. Wang, Alamusi, N. Hu, *Sci. Rep.*, 4 (2014) 4518.
20. X. Zhao, Y. Du, L. Jin, Y. Yang, S. Wu, W. Li, Y. Yu, *Sci. Rep.*, 5 (2015) 14146.
21. C.Z. Yuan, B. Gao, L.F. Shen, S.D. Yang, L. Hao, *Nanoscale.*, 3 (2011) 529.
22. H.R. Naderi, H.R. Mortaheb, A. Zolfaghari, *J. Electroanal. Chem.*, 719 (2014) 98.
23. B. Gnana Sundara Raj, A.M. Asiri, A.H. Qusti, *Ultrason. Sonochem.*, 21 (2014) 1933.

24. Y.X. Zhang, M. Huang, F. Li, X.L. Wang, Z.Q. Wen, *J. Power Sources.*, 246 (2014) 449.
25. R.N. Reddy, R.G. Reddy., *J. Power Sources.*, 132 (2004) 315.
26. H.U. Shah, F. Wang, M.S. Javed, N. Shaheen, Y. Ye, *J. Alloys Compd.*, 725 (2017) 1223.